

Role of double TiO_2 layers at the interface of $\text{FeSe}/\text{SrTiO}_3$ superconductors

Ke Zou,^{1,2} Subhasish Mandal,^{1,2} Stephen D. Albright,^{2,3} Rui Peng,⁴ Yujia Pu,⁴ Divine Kumah,^{1,2} Claudia Lau,^{2,3} Georg H. Simon,^{2,5} Omur E. Dagdeviren,^{2,5} Xi He,^{1,6} Ivan Božović,^{1,6} Udo D. Schwarz,^{2,5,7} Eric I. Altman,^{2,7} Donglai Feng,⁴ Fred J. Walker,^{1,2} Sohrab Ismail-Beigi,^{1,2} and Charles H. Ahn^{1,2,3,5}

¹Department of Applied Physics, Yale University, New Haven, Connecticut 06520, USA

²Center for Research on Interface Structures and Phenomena (CRISP), Yale University, New Haven, Connecticut 06520, USA

³Department of Physics, Yale University, New Haven, Connecticut 06520, USA

⁴State Key Laboratory of Surface Physics, Department of Physics and Advanced Materials Laboratory, Fudan University, Shanghai 200433, China

⁵Department of Mechanical Engineering and Materials Science, Yale University, New Haven, Connecticut 06520, USA

⁶Condensed Matter Physics and Materials Science Department, Brookhaven National Laboratory, Upton, New York 11973, USA

⁷Department of Chemical and Environmental Engineering, Yale University, New Haven, Connecticut 06520, USA

(Received 19 November 2015; revised manuscript received 29 April 2016; published 16 May 2016)

We determine the surface reconstruction of SrTiO_3 used to achieve superconducting FeSe films in experiments, which is different from the 1×1 TiO_2 -terminated SrTiO_3 assumed by most previous theoretical studies. In particular, we identify the existence of a double TiO_2 layer at the $\text{FeSe}/\text{SrTiO}_3$ interface that plays two important roles. First, it facilitates the epitaxial growth of FeSe . Second, *ab initio* calculations reveal a strong tendency for electrons to transfer from an oxygen deficient SrTiO_3 surface to FeSe when the double TiO_2 layer is present. The double layer helps to remove the hole pocket in the FeSe at the Γ point of the Brillouin zone and leads to a band structure characteristic of superconducting samples. The characterization of the interface structure presented here is a key step towards the resolution of many open questions about this superconductor.

DOI: 10.1103/PhysRevB.93.180506

The discovery of the iron-based superconductors (SCs) [1–14] exhibiting unconventional superconductivity promises to enhance our understanding of superconductivity and leads to the development of new materials with high critical temperature (T_c). Iron pnictides [15–18] and chalcogenides [1–14,19–33], the simplest being LiFeAs ($T_c = 18$ K) [34–36] and FeSe ($T_c = 9$ K) [1], respectively, share important similarities with cuprate superconductors [37,38]. Both possess a two-dimensional layered structure and exhibit antiferromagnetic ordering or other ordering (such as nematic ordering) at low temperatures that competes with superconducting phases. They also show enhanced superconductivity when dopants are added to their layered structures (e.g., hole doping of CuO planes in $\text{YBa}_2\text{Cu}_3\text{O}_{7-x}$ [38], doping of FeAs planes in $\text{SmFeAsO}_{1-x}\text{F}_x$ [17], and K doping in bulk planar FeSe superconductors [31]).

A particularly intriguing Fe-based SC is one-unit-cell (1-u.c.) FeSe grown on SrTiO_3 (STO) substrates via molecular beam epitaxy, with a reported [12] T_c above 100 K, the highest among Fe-based SCs and rivaled only by a few cuprates [37,38] and H_2S under extreme pressure [39]. This surprising enhancement of T_c in 1-u.c. FeSe/STO compared to the bulk phase [40,41] has been ascribed to interactions between FeSe and STO due to the interfacial nature of the system. The 1-u.c. FeSe grown on BaTiO_3 [9] and on anatase TiO_2 [42] also shows enhanced T_c . All three substrates are terminated with TiO_2 layers. The mechanism for Cooper pairing in this material is an active area of investigation, and a deeper understanding of the interactions between FeSe and STO may provide insight into the origins of unconventional SCs.

In this Rapid Communication, we experimentally determine the atomic structure of 1-u.c. FeSe/STO and use density functional theory to explore how it affects the electronic

structure. Specifically, we identify an STO surface reconstruction that is not a simple truncation of the bulk structure, but represents a change in interface stoichiometry, whereby the STO terminates with two monolayers (2 ML) of TiO_2 . We show that this reconstruction is critical in two ways. First, it facilitates the growth of coherently strained, epitaxial FeSe . Second, the 2 ML TiO_2 -terminated surface facilitates electron transfer to FeSe by modifying both the electronic structure and defect chemistry at the FeSe/STO interface. The importance of a reconstructed surface has been suggested to be the key to achieving high T_c in this materials system [4,25,28,32], but so far has not been included in theoretical attempts to account for enhanced superconductivity in 1-u.c. FeSe/STO .

The growth procedures of the FeSe/STO are similar to those reported in Refs. [5,8,10,12,25,28]. The STO substrates are prepared using a high-temperature (950 °C) anneal in air at ambient pressure by using the procedures described in Refs. [5,8]. In addition, bulk STO substrates terminated with a single TiO_2 layer are prepared using a standard etch procedure [43]. The substrates are annealed in flowing oxygen at approximately 1000 °C, as described in Sec. 1 of the Supplemental Material [44].

Similar high-temperature annealing usually leads to a 2 ML TiO_2 surface termination with various reconstructions [45–48]. We confirm the existence of 2 ML TiO_2 using synchrotron x-ray diffraction. The experiments are performed in vacuum at 300 K at the 33ID beam line at the Advanced Photon Source with an incident x-ray wavelength of 0.83 Å (15 keV). The $(2,0,\ell)$ crystal truncation rod measured for STO is shown in Fig. 1(a), together with a fit to a model of a 2 ML TiO_2 surface termination. Note that the rods of 1×1 1 ML TiO_2 -terminated STO show features distinct from the 2 ML TiO_2 -terminated STO, as shown in Sec. 4 of the Supplemental Material [44].

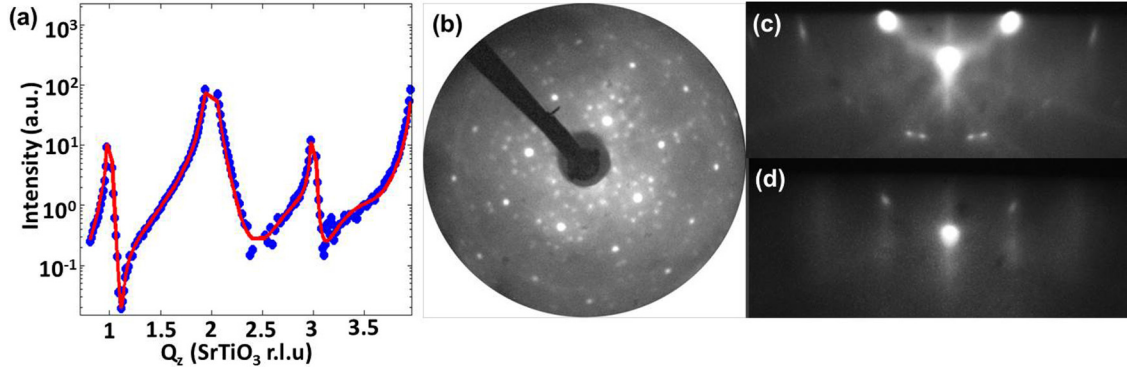


FIG. 1. Identification of 2 ML TiO_2 on STO and the epitaxial growth of 1×1 FeSe. (a) $(2,0,\ell)$ crystal truncation rod (CTR) of a treated STO substrate (blue circles). Red line is a fit using a 2 ML surface model. (b) and (c) Low-energy electron diffraction (LEED) and reflection high-energy electron diffraction (RHEED) of STO substrates showing the $\sqrt{13} \times \sqrt{13}$ $R33.7^\circ$ reconstruction. (d) RHEED of 1-u.c. FeSe on STO showing the 1×1 structure of the FeSe.

Subsequent experiments reveal that the annealing results in a highly ordered $\sqrt{13} \times \sqrt{13}$ $R33.7^\circ$ reconstruction, easily identified by the sharp diffraction features in synchrotron x-ray diffraction [Fig. 2(a)], low-energy electron diffraction (LEED) [Fig. 1(b)], and reflection high-energy electron diffraction (RHEED) [Fig. 1(c)]. This RHEED pattern is strikingly similar to those shown in prior reports [25,28,32] of 1-u.c. FeSe/STO, though the nature of the reconstruction is not identified.

By comparing FeSe growth on STO substrates with the two different types of termination, we establish that a 2 ML TiO_2 -terminated STO surface promotes the epitaxial growth of FeSe. After preparing the 2 ML TiO_2 surface, samples are loaded for chalcogenide molecular beam epitaxy (MBE) growth. Before growth, the substrates are treated by high-temperature vacuum and Se annealing that leads to a less ordered surface reconstruction while retaining the 2 ML TiO_2 termination. The substrates are cooled to a growth temperature of $\sim 450\text{--}500\text{ }^\circ\text{C}$. The 1-u.c. FeSe films grown on such reconstructed surfaces are epitaxial and coherently strained, as indicated by RHEED [Fig. 1(d)]. Note that the RHEED for the 1-u.c. FeSe films has a 1×1 pattern, which is the same symmetry as that

observed in 1 ML TiO_2 -terminated STO substrates, i.e., it does not show the $\sqrt{13} \times \sqrt{13}$ reconstruction that is apparent in RHEED from the 2 ML TiO_2 -terminated STO substrate just before growth [Fig. 1(c)]. However, synchrotron x-ray diffraction indicates that, even after deposition of FeSe, the $\sqrt{13} \times \sqrt{13}$ reconstruction of the STO is still present under FeSe [Fig. 2(a)]. Growth on surfaces terminated with a single layer of TiO_2 under a range of conditions results in films that show diffuse RHEED patterns, indicative of disordered films (Figs. S1 and S3) [44].

To examine the electronic structure of the samples, we carry out *in situ*, low-temperature angle-resolved photoemission spectroscopy (ARPES) on 1-u.c. FeSe grown on a 2 ML TiO_2 -terminated STO [5,8]. Data taken near the M point of the Brillouin zone are shown in Fig. 2(b). At $T = 25\text{ K}$, an electron band is observed at the M point, as in other reports [5,27,28] of superconducting 1-u.c. FeSe/STO. Figure 2(c) shows symmetrized photoemission spectra [energy distribution curves (EDCs)] across the Fermi level for the area marked by the red box in Fig. 2(b). The opening of a gap is indicated by a dip at the Fermi level in the EDCs and by the inflection of

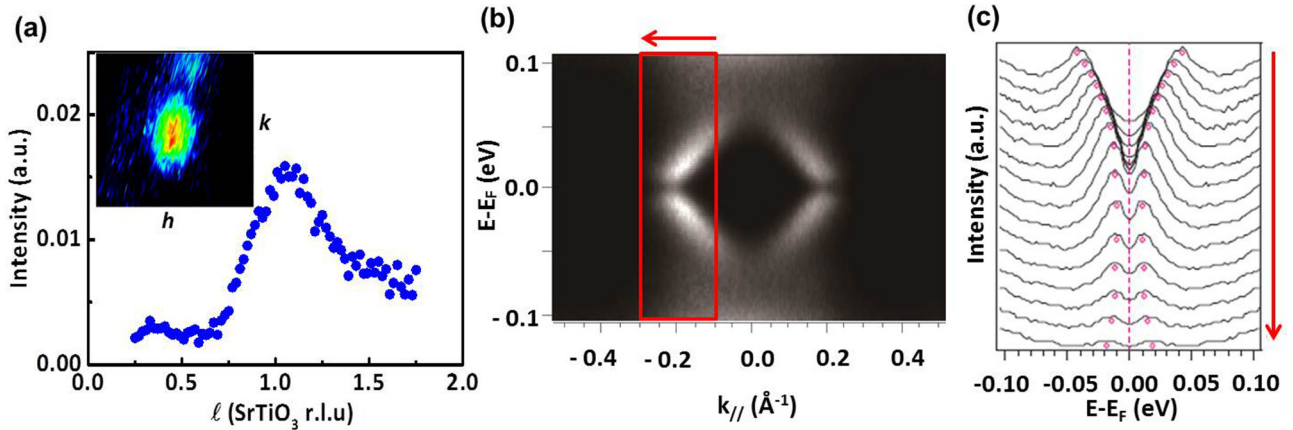


FIG. 2. 1-u.c. FeSe/STO with 2 ML TiO_2 at the interface. (a) Crystal truncation rod along $(2/13, 10/13, \ell)$ of FeSe/STO. Inset: Reciprocal space mapping around the $(2/13, 10/13, 0.8)$ peak. Ranges of h and k in the inset are 0.1 with a unit of 13 r.l.u. Both plots indicate that the $\sqrt{13} \times \sqrt{13}$ reconstruction of STO remains beneath FeSe. (b) ARPES intensity near the M point at the corner of the Brillouin zone. To highlight the gap at the Fermi level, the data above the Fermi level are the mirror images of the data below the Fermi level. (c) Symmetrized energy distribution curves along the portion indicated by the red box and arrow in (b).

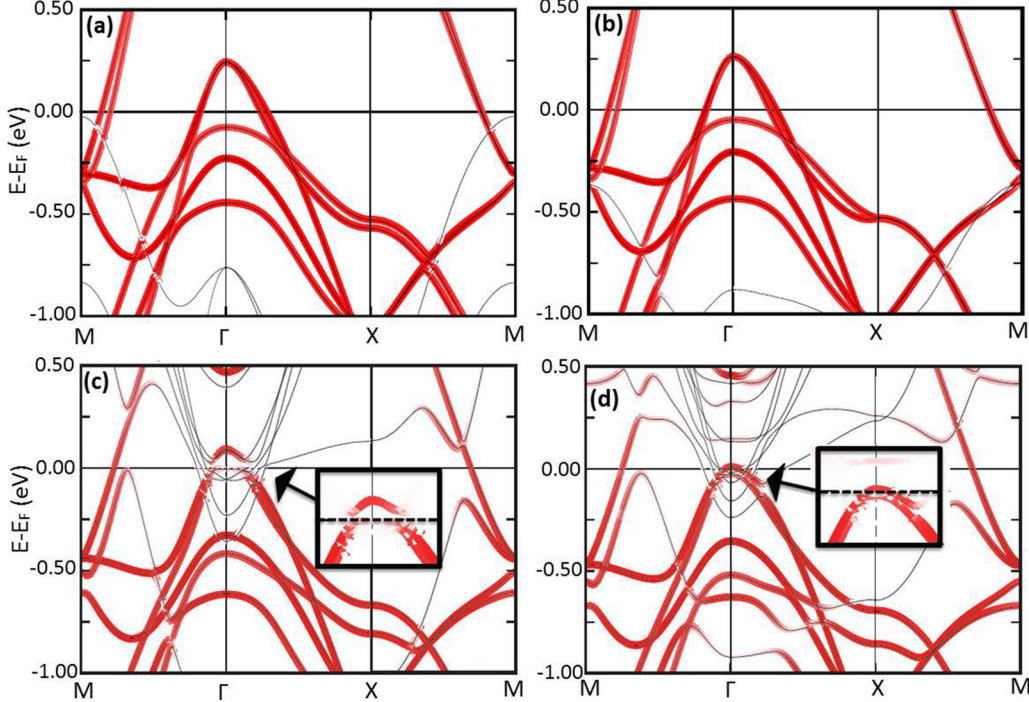


FIG. 3. Orbitally resolved band structures for Fe 3d for four models of 1-u.c. FeSe/STO: (a) with stoichiometric 1 ML TiO₂ termination, (b) with stoichiometric 2 ML termination, (c) with 1 ML termination and 50% oxygen vacancies, and (d) with 2 ML termination and 50% oxygen vacancies. Thin black lines represent the electron energy bands for the entire heterostructure; the red overlay represents projections of the Fe 3d orbital, where the color intensity is proportional to the projection amount. Fermi level is at zero in all cases. Energy scale is in eV. Insets in (c) and (d): Zoom-in on the Fe bands around the Γ point.

the quasiparticle dispersion near the Fermi level, as marked by the red symbols [Fig. 2(c)] [5,27,28]. From these data we conclude that a 2 ML TiO₂-terminated STO substrate supports the electronic structure characteristic of superconducting FeSe.

To explore the role of the 2 ML TiO₂ interface on the electronic structure of 1-u.c. FeSe/STO, we compute the band structure using density functional theory (DFT) for FeSe on 1 ML and 2 ML TiO₂-terminated STO [44]. A significant feature of the ARPES spectra in superconducting 1-u.c. FeSe, unlike in bulk FeSe, is the absence of a hole pocket at the Γ point and the presence of an electron band at the M point [see Fig. 2(b)] [5,27,28]. We find that a 2 ML TiO₂-terminated STO surface promotes charge transfer and can suppress this feature of the electronic structure more effectively than a 1 ML TiO₂ termination. The band structures of ideal 1-u.c. FeSe/STO with 1 ML and 2 ML TiO₂ terminations are shown in Figs. 3(a) and 3(b), respectively. Both ideal terminations have similar band structures with a prominent hole pocket predicted around Γ , which is absent in the experiments; electron transfer to the FeSe is required to fill this pocket. The prime candidate source of electrons comes from oxygen vacancies in the STO surface layers [4,5,49], a mechanism we explore below, although other defects could play a role as well [50].

With this motivation, we have performed DFT calculations for interfaces with 50% O vacancies in the surface layer of STO for both the 1 ML and 2 ML TiO₂ terminations. The removal of oxygen results in a significant structural and energetic change at the interface. Similar results are reported in Ref. [4]. The ideal stoichiometric STO surfaces bond weakly to the FeSe, with Ti-Se distances of 3.11 and 3.50 Å in the 1 ML and 2 ML

configurations, along with extremely weak binding energies of 0.073 and 0.089 eV per Ti-Se bond. The introduction of O vacancies shortens and greatly strengthens the bonds: The Ti-Se distances become 2.82 and 2.67 Å in the 1 ML and 2 ML cases, respectively, with sizable binding energies of 0.60 and 0.88 eV per Ti-Se bond. The 2 ML TiO₂ geometry with vacancies displays stronger binding and thus further promotes epitaxy. A similar enhancement of bonding along with smaller Se-Ti distances of 2.6 and 2.9 Å in the 1 ML geometry has been reported [4,50]. We note all the calculated Se-Ti distances are smaller than the available experimental value [51]. One reason for the discrepancy may be that far fewer O vacancies are present in the experimental system, which will generally reduce charge transfer and decrease the binding.

The stronger binding in the 2 ML case goes hand in hand with stronger electron doping from STO to FeSe [Figs. S4(a)–S4(d) show the electron transfer [44]], which moves the FeSe Fermi level up in energy [see Figs. 3(c) and 3(d)]. In the 2 ML termination, this doping removes the hole pocket at the Γ point, recovering the band structure observed in ARPES. For the same vacancy concentration, the 1 ML system still has a noticeable hole pocket at Γ [compare Figs. 3(c) and 3(d)]. One simple reason for the enhanced 2 ML electron transfer is that the electrons are already more effectively confined near the surface in the case of 2 ML TiO₂ termination (see Fig. S5 for details [44]), while in the 1 ML termination, some of the electrons near the surface “leak back” into the STO substrate and are unavailable for transfer into the FeSe.

We have also computed the consequence of having a very high oxygen vacancy concentration of 100% on the 1 × 1

TABLE I. Relative oxygen vacancy formation energy on the surface of SrTiO_3 with respect to 1×1 geometry as a function of surface unit cell and vacancy concentration.

Surface unit cell	% vacancy concentration	Vacancy formation energy (eV)	
		1 ML TiO_2	2 ML TiO_2
1×1	50	0	-0.22
$c(2 \times 2)$	50	-0.01	-0.17
2×2	12.5	-0.70	-1.54

1 ML TiO_2 and 2 ML TiO_2 surfaces. In both cases, the added electrons stay in the STO and do not transfer to the FeSe subsystem: As expected, there is a limit to the electron transfer and beyond 50% vacancy concentration no further electrons dope the FeSe. Hence, we conclude that removal of the hole pocket at Γ requires some type of surface reconstruction beyond the 1×1 1 ML TiO_2 structure. One possibility [4] is to have 50% O vacancies and a 2×1 reconstruction of the 1 ML TiO_2 surface, which removes the hole pocket at Γ . However, the experimentally observed STO surface corresponds to a 2 ML TiO_2 reconstruction, which is also effective at removing the hole pocket with 50% O vacancies.

Energetically, it is more favorable to have high oxygen vacancy concentrations in the 2 ML TiO_2 structure compared to the 1 ML TiO_2 termination. Table I shows the DFT-computed vacancy formation energy (VFE), which is the energy cost of removing an oxygen atom from the STO surface and moving it far into the vacuum. In every case, the VFE is more favorable for the 2 ML termination than the 1 ML termination. For reference, the VFE on the 2 ML surface is lower than that inside the STO films by 0.25 eV.

To check consistency between ARPES and DFT results for electron transfer, we have integrated the DFT densities of states to find that 0.26 electrons per Fe are needed to fill the hole pocket at Γ of an FeSe monolayer. These electrons fill the hole pocket at Γ and also the electron pocket about M . The DFT band structure shows that the Fermi wave vectors for both pockets are very close in magnitude, so we expect ~ 0.13 electrons per Fe for each pocket separately. We are gratified that prior high-resolution ARPES measurements on identically prepared samples [5] estimate ~ 0.12 electrons per Fe from measurement of the Fermi surface about the M point.

In bulk FeSe and other iron pnictides, the bond angle $X\text{-Fe-}X$ ($X = \text{As, Se, ...}$) and the $X\text{-Fe}$ height control the strength of electron-electron correlations and other properties such as T_c [52–54]. It has been shown when the As-Fe-As bond angle ranges from 106° to 114° , the T_c is greatly enhanced in various pnictide superconductors [55]. For 1-u.c. FeSe/STO, the Se-Fe-Se bond angle in our DFT calculation is

115.1° , compared with the experimental results of 111.9° [51]. Both values are close to the range of 106° – 114° , within which the electron-electron correlations are considered to be important [55], which may explain the difference between our DFT and the experimental values.

The most straightforward consequence of the structure determined here is that the electron transfer to the FeSe is enhanced by the 2 ML TiO_2 termination more strongly than by other surface structures of STO. The enhanced electron transfer completely suppresses the hole pocket near the Γ point and only Fermi-level crossings near the M point remain [Fig. 2(b)], which is the band structure that is generally believed to be a requirement [5,27,28] for superconducting 1-u.c. FeSe/STO. Doping of the FeSe is an important aspect of the physics of FeSe/STO heterostructures. In Fe-based SCs, as well as in the cuprates, the superconducting phase competes with magnetic phases. For example, based on photoemission measurements, spin density waves (SDWs) in thin FeSe films are suppressed by heavy electron doping, promoting the superconducting phase [5]. Several mechanisms have been proposed to explain the enhanced superconductivity in 1-u.c. FeSe/STO. An optimized doping level in FeSe may be achieved due to the stronger bonding and interfacial electron transfer. This tighter STO-FeSe coupling may also impose a more robust epitaxial constraint that could lead to a structure predicted to open strong electron-phonon coupling channels not present in the bulk [30].

To summarize, we identify the existence of double TiO_2 layers at the surface of STO within 1-u.c. FeSe/STO films. The double TiO_2 layers play a key role in the epitaxial growth of FeSe, facilitating electron transfer between FeSe and STO and suppressing the hole pocket at the Γ point. This work provides compelling evidence that the electron transfer facilitated by the 2 ML TiO_2 termination is critical for superconductivity in 1-u.c. FeSe/STO.

This research is sponsored by the DMR NSF MRSEC 1119826 and the AFOSR under Grant No. FA9550-15-1-0472. R.P., Y.P., and D.F. acknowledge support from the National Science Foundation of China, and the National Basic Research Program of China (973 Program) under Grant No. 2012CB921402. The work at Argonne National Laboratory is supported by the US Department of Energy. Magnetic measurements (X.H. and I.B.) at BNL were supported by the US Department of Energy, Basic Energy Sciences, Materials Sciences and Engineering Division. Computational facilities are supported by NSF Grant No. CNS 08-21132 and by the facilities and staff of the Yale University Faculty of Arts and Sciences High Performance Computing Center. Additional computations were carried out via the NSF XSEDE resources through Grant No. TG-MCA08 x 007.

[1] F.-C. Hsu, J.-Y. Luo, K.-W. Yeh, T.-K. Chen, T.-W. Huang, P. M. Wu, Y.-C. Lee, Y.-L. Huang, Y.-Y. Chu, D.-C. Yan, and M.-K. Wu, Superconductivity in the PbO-type structure α -FeSe, *Proc. Natl. Acad. Sci. U.S.A.* **105**, 14262 (2008).

[2] Y. Zhang, L. X. Yang, M. Xu, Z. R. Ye, F. Chen, C. He, H. C. Xu, J. Jiang, B. P. Xie, J. J. Ying, X. F. Wang, X. H. Chen, J. P. Hu, M. Matsunami, S. Kimura, and D. L. Feng, Nodeless superconducting gap in $A_x\text{Fe}_2\text{Se}_2$ ($A = \text{K, Cs}$) revealed by

- angle-resolved photoemission spectroscopy, *Nat. Mater.* **10**, 273 (2011).
- [3] Y. Lubashevsky, E. Lahoud, K. Chashka, D. Podolsky, and A. Kanigel, Shallow pockets and very strong coupling superconductivity in FeSe_xTe_{1-x}, *Nat. Phys.* **8**, 309 (2012).
- [4] J. Bang, Z. Li, Y. Y. Sun, A. Samanta, Y. Y. Zhang, W. H. Zhang, L. L. Wang, X. Chen, X. C. Ma, Q. K. Xue, and S. B. Zhang, Atomic and electronic structures of single-layer FeSe on SrTiO₃(001): The role of oxygen deficiency, *Phys. Rev. B* **87**, 220503 (2013).
- [5] S. Tan, Y. Zhang, M. Xia, Z. Ye, F. Chen, X. Xie, R. Peng, D. Xu, Q. Fan, H. Xu, J. Jiang, T. Zhang, X. Lai, T. Xiang, J. Hu, B. Xie, and D. Feng, Interface-induced superconductivity and strain-dependent spin density waves in FeSe/SrTiO₃ thin films, *Nat. Mater.* **12**, 634 (2013).
- [6] I. Bozovic and C. Ahn, A new frontier for superconductivity, *Nat. Phys.* **10**, 892 (2014).
- [7] S. Mandal, R. E. Cohen, and K. Haule, Strong pressure-dependent electron-phonon coupling in FeSe, *Phys. Rev. B* **89**, 220502 (2014).
- [8] R. Peng, X. P. Shen, X. Xie, H. C. Xu, S. Y. Tan, M. Xia, T. Zhang, H. Y. Cao, X. G. Gong, J. P. Hu, B. P. Xie, and D. L. Feng, Measurement of an Enhanced Superconducting Phase and a Pronounced Anisotropy of the Energy Gap of a Strained FeSe Single Layer in FeSe/Nb:SrTiO₃/KTaO₃ Heterostructures Using Photoemission Spectroscopy, *Phys. Rev. Lett.* **112**, 107001 (2014).
- [9] R. Peng, H. C. Xu, S. Y. Tan, H. Y. Cao, M. Xia, X. P. Shen, Z. C. Huang, C. H. P. Wen, Q. Song, T. Zhang, B. P. Xie, X. G. Gong, and D. L. Feng, Tuning the band structure and superconductivity in single-layer FeSe by interface engineering, *Nat. Commun.* **5**, 5044 (2014).
- [10] Y. Sun, W. Zhang, Y. Xing, F. Li, Y. Zhao, Z. Xia, L. Wang, X. Ma, Q.-K. Xue, and J. Wang, High temperature superconducting FeSe films on SrTiO₃ substrates, *Sci. Rep.* **4**, 6040 (2014).
- [11] Q. Fan, W. H. Zhang, X. Liu, Y. J. Yan, M. Q. Ren, R. Peng, H. C. Xu, B. P. Xie, J. P. Hu, T. Zhang, and D. L. Feng, Plain *s*-wave superconductivity in single-layer FeSe on SrTiO₃ probed by scanning tunneling microscopy, *Nat. Phys.* **11**, 946 (2015).
- [12] J.-F. Ge, Z.-L. Liu, C. Liu, C.-L. Gao, D. Qian, Q.-K. Xue, Y. Liu, and J.-F. Jia, Superconductivity above 100 K in single-layer FeSe films on doped SrTiO₃, *Nat. Mater.* **14**, 285 (2015).
- [13] D. Huang, C.-L. Song, T. A. Webb, S. Fang, C.-Z. Chang, J. S. Moodera, E. Kaxiras, and J. E. Hoffman, Revealing the Empty-State Electronic Structure of Single-Unit-Cell FeSe/SrTiO₃, *Phys. Rev. Lett.* **115**, 017002 (2015).
- [14] M. K. Wu, P. M. Wu, Y. C. Wen, M. J. Wang, P. H. Lin, W. C. Lee, T. K. Chen, and C. C. Chang, An overview of the Fe-chalcogenide superconductors, *J. Phys. D: Appl. Phys.* **48**, 323001 (2015).
- [15] S. Lee, C. Tarantini, P. Gao, J. Jiang, J. D. Weiss, F. Kametani, C. M. Folkman, Y. Zhang, X. Q. Pan, E. E. Hellstrom, D. C. Larbalestier, and C. B. Eom, Artificially engineered superlattices of pnictide superconductors, *Nat. Mater.* **12**, 392 (2013).
- [16] Y. Mizukami, M. Konczykowski, Y. Kawamoto, S. Kurata, S. Kasahara, K. Hashimoto, V. Mishra, A. Kreisel, Y. Wang, P. J. Hirschfeld, Y. Matsuda, and T. Shibauchi, Disorder-induced topological change of the superconducting gap structure in iron pnictides, *Nat. Commun.* **5**, 5657 (2014).
- [17] X. H. Chen, T. Wu, G. Wu, R. H. Liu, H. Chen, and D. F. Fang, Superconductivity at 43 K in SmFeAsO_{1-x}F_x, *Nature (London)* **453**, 761 (2008).
- [18] Y. Kamihara, T. Watanabe, M. Hirano, and H. Hosono, Iron-based layered superconductor LaO_{1-x}F_xFeAs ($x = 0.05\text{--}0.12$) with $T_c = 26$ K, *J. Am. Chem. Soc.* **130**, 3296 (2008).
- [19] Y. Mizuguchi, F. Tomioka, S. Tsuda, T. Yamaguchi, and Y. Takano, Superconductivity at 27 K in tetragonal FeSe under high pressure, *Appl. Phys. Lett.* **93**, 152505 (2008).
- [20] T. Imai, K. Ahilan, F. L. Ning, T. M. McQueen, and R. J. Cava, Why Does Undoped FeSe Become a High- T_c Superconductor under Pressure?, *Phys. Rev. Lett.* **102**, 177005 (2009).
- [21] T. M. McQueen, A. J. Williams, P. W. Stephens, J. Tao, Y. Zhu, V. Ksenofontov, F. Casper, C. Felser, and R. J. Cava, Tetragonal-to-Orthorhombic Structural Phase Transition at 90 K in the Superconductor Fe_{1.01}Se, *Phys. Rev. Lett.* **103**, 057002 (2009).
- [22] S. Medvedev, T. M. McQueen, I. A. Troyan, T. Palasyuk, M. I. Eremets, R. J. Cava, S. Naghavi, F. Casper, V. Ksenofontov, G. Wortmann, and C. Felser, Electronic and magnetic phase diagram of beta-Fe_{1.01}Se with superconductivity at 36.7 K under pressure, *Nat. Mater.* **8**, 630 (2009).
- [23] J. Guo, S. Jin, G. Wang, S. Wang, K. Zhu, T. Zhou, M. He, and X. Chen, Superconductivity in the iron selenide K_xFe₂Se₂ ($0 \leq x \leq 1.0$), *Phys. Rev. B* **82**, 180520 (2010).
- [24] D. Liu, W. Zhang, D. Mou, J. He, Y.-B. Ou, Q.-Y. Wang, Z. Li, L. Wang, L. Zhao, S. He, Y. Peng, X. Liu, C. Chen, L. Yu, G. Liu, X. Dong, J. Zhang, C. Chen, Z. Xu, J. Hu, X. Chen, X. Ma, Q. Xue, and X. J. Zhou, Electronic origin of high-temperature superconductivity in single-layer FeSe superconductor, *Nat. Commun.* **3**, 931 (2012).
- [25] Q.-Y. Wang, Z. Li, W.-H. Zhang, Z.-C. Zhang, J.-S. Zhang, W. Li, H. Ding, Y.-B. Ou, P. Deng, K. Chang, J. Wen, C.-L. Song, K. He, J.-F. Jia, S.-H. Ji, Y.-Y. Wang, L.-L. Wang, X. Chen, X.-C. Ma, and Q.-K. Xue, Interface-induced high-temperature superconductivity in single unit-cell FeSe films on SrTiO₃, *Chin. Phys. Lett.* **29**, 037402 (2012).
- [26] Y.-Y. Xiang, F. Wang, D. Wang, Q.-H. Wang, and D.-H. Lee, High-temperature superconductivity at the FeSe/SrTiO₃ interface, *Phys. Rev. B* **86**, 134508 (2012).
- [27] S. He, J. He, W. Zhang, L. Zhao, D. Liu, X. Liu, D. Mou, Y.-B. Ou, Q.-Y. Wang, Z. Li, L. Wang, Y. Peng, Y. Liu, C. Chen, L. Yu, G. Liu, X. Dong, J. Zhang, C. Chen, Z. Xu, X. Chen, X. Ma, Q. Xue, and X. J. Zhou, Phase diagram and electronic indication of high-temperature superconductivity at 65 K in single-layer FeSe films, *Nat. Mater.* **12**, 605 (2013).
- [28] J. J. Lee, F. T. Schmitt, R. G. Moore, S. Johnston, Y. T. Cui, W. Li, M. Yi, Z. K. Liu, M. Hashimoto, Y. Zhang, D. H. Lu, T. P. Devoreaux, D. H. Lee, and Z. X. Shen, Interfacial mode coupling as the origin of the enhancement of T_c in FeSe films on SrTiO₃, *Nature (London)* **515**, 245 (2014).
- [29] W.-H. Zhang, Y. Sun, J.-S. Zhang, F.-S. Li, M.-H. Guo, Y.-F. Zhao, H.-M. Zhang, J.-P. Peng, Y. Xing, H.-C. Wang, T. Fujita, A. Hirata, Z. Li, H. Ding, C.-J. Tang, M. Wang, Q.-Y. Wang, K. He, S.-H. Ji, X. Chen, J.-F. Wang, Z.-C. Xia, L. Li, Y.-Y. Wang, J. Wang, L.-L. Wang, M.-W. Chen, Q.-K. Xue, and X.-C. Ma, Direct observation of high-temperature superconductivity in one-unit-cell FeSe films, *Chin. Phys. Lett.* **31**, 017401 (2014).

- [30] S. Coh, M. L. Cohen, and S. G. Louie, Large electron-phonon interactions from FeSe phonons in a monolayer, *New J. Phys.* **17**, 073027 (2015).
- [31] Y. Miyata, K. Nakayama, K. Sugawara, T. Sato, and T. Takahashi, High-temperature superconductivity in potassium-coated multilayer FeSe thin films, *Nat. Mater.* **14**, 775 (2015).
- [32] F. S. Li, H. Ding, C. J. Tang, J. P. Peng, Q. H. Zhang, W. H. Zhang, G. Y. Zhou, D. Zhang, C. L. Song, K. He, S. H. Ji, X. Chen, L. Gu, L. L. Wang, X. C. Ma, and Q. K. Xue, Interface-enhanced high-temperature superconductivity in single-unit-cell $\text{FeTe}_{1-x}\text{Se}_x$ films on SrTiO_3 , *Phys. Rev. B* **91**, 220503 (2015).
- [33] X. Liu, D. Liu, W. Zhang, J. He, L. Zhao, S. He, D. Mou, F. Li, C. Tang, Z. Li, L. Wang, Y. Peng, Y. Liu, C. Chen, L. Yu, G. Liu, X. Dong, J. Zhang, C. Chen, Z. Xu, X. Chen, X. Ma, Q. Xue, and X. J. Zhou, Dichotomy of the electronic structure and superconductivity between single-layer and double-layer FeSe/ SrTiO_3 films, *Nat. Commun.* **5**, 5047 (2014).
- [34] J. H. Tapp, Z. J. Tang, B. Lv, K. Sasmal, B. Lorenz, P. C. W. Chu, and A. M. Guloy, LiFeAs: An intrinsic FeAs-based superconductor with $T_c = 18\text{ K}$, *Phys. Rev. B* **78**, 060505 (2008).
- [35] X. C. Wang, Q. Q. Liu, Y. X. Lv, W. B. Gao, L. X. Yang, R. C. Yu, F. Y. Li, and C. Q. Jin, The superconductivity at 18 K in LiFeAs system, *Solid State Commun.* **148**, 538 (2008).
- [36] K. Ishida, Y. Nakai, and H. Hosono, To what extent iron-pnictide new superconductors have been clarified: A progress report, *J. Phys. Soc. Jpn.* **78**, 062001 (2009).
- [37] E. Dagotto, Correlated Electrons In High-temperature superconductors, *Rev. Mod. Phys.* **66**, 763 (1994).
- [38] P. A. Lee, N. Nagaosa, and X. G. Wen, Doping a Mott insulator: Physics of high-temperature superconductivity, *Rev. Mod. Phys.* **78**, 17 (2006).
- [39] A. P. Drozdov, M. I. Eremets, I. A. Troyan, V. Ksenofontov, and S. I. Shylin, Conventional superconductivity at 203 kelvin at high pressures in the sulfur hydride system, *Nature (London)* **525**, 73 (2015).
- [40] C. L. Song, Y. L. Wang, P. Cheng, Y. P. Jiang, W. Li, T. Zhang, Z. Li, K. He, L. L. Wang, J. F. Jia, H. H. Hung, C. J. Wu, X. C. Ma, X. Chen, and Q. K. Xue, Direct observation of nodes and twofold symmetry in FeSe superconductor, *Science* **332**, 1410 (2011).
- [41] C. L. Song, Y. L. Wang, Y. P. Jiang, Z. Li, L. L. Wang, K. He, X. Chen, X. C. Ma, and Q. K. Xue, Molecular-beam epitaxy and robust superconductivity of stoichiometric FeSe crystalline films on bilayer graphene, *Phys. Rev. B* **84**, 020503 (2011).
- [42] H. Ding, Y. F. Lv, K. Zhao, W. L. Wang, L. L. Wang, C. L. Song, X. Chen, X. C. Ma, and Q. K. Xue, High-temperature superconductivity in single-unit-cell FeSe films on anatase $\text{TiO}_2(001)$, *arXiv:1603.00999*.
- [43] M. Kareev, S. Prosandeev, J. Liu, C. Gan, A. Kareev, J. W. Freeland, M. Xiao, and J. Chakhalian, Atomic control and characterization of surface defect states of TiO_2 terminated SrTiO_3 single crystals, *Appl. Phys. Lett.* **93**, 061909 (2008).
- [44] See Supplemental Material at <http://link.aps.org/supplemental/10.1103/PhysRevB.93.180506> for a description of further details related to sample preparation methods, density functional theory calculations, RHEED of FeSe grown on $1 \times 1 1$ ML TiO_2 -terminated SrTiO_3 , comparison of crystal truncation rods of 1 ML and 2 ML TiO_2 -terminated SrTiO_3 , intensity of RHEED patterns of SrTiO_3 and FeSe films, and electron transfer and density of states at FeSe/ SrTiO_3 interfaces.
- [45] N. Erdman and L. D. Marks, $\text{SrTiO}(001)$ surface structures under oxidizing conditions, *Surf. Sci.* **526**, 107 (2003).
- [46] O. Warschkow, M. Asta, N. Erdman, K. R. Poeppelmeier, D. E. Ellis, and L. D. Marks, TiO_2 -rich reconstructions of $\text{SrTiO}_3(001)$: a theoretical study of structural patterns, *Surf. Sci.* **573**, 446 (2004).
- [47] D. M. Kienzle, A. E. Becerra-Toledo, and L. D. Marks, Vacant-Site Octahedral Tilings on SrTiO_3 (001), the $(\sqrt{13} \times \sqrt{13})R33.7^\circ$ Surface, and Related Structures, *Phys. Rev. Lett.* **106**, 176102 (2011).
- [48] O. E. Dagdeviren, G. H. Simon, K. Zou, F. J. Walker, C. Ahn, E. I. Altman, and U. D. Schwarz, Surface phase, morphology, and charge distributions on vacuum and ambient annealed SrTiO_3 (100), *Phys. Rev. B* **93**, 195303 (2016).
- [49] H. Y. Cao, S. Y. Tan, H. J. Xiang, D. L. Feng, and X. G. Gong, Interfacial effects on the spin density wave in FeSe/ SrTiO_3 thin films, *Phys. Rev. B* **89**, 014501 (2014).
- [50] K. V. Shanavas and D. J. Singh, Doping SrTiO_3 supported FeSe by excess atoms and oxygen vacancies, *Phys. Rev. B* **92**, 035144 (2015).
- [51] F. Li, Q. Zhang, C. Tang, C. Liu, J. Shi, C. Nie, G. Zhou, Z. Li, W. Zhang, C. L. Song, K. He, S. Ji, S. Zhang, L. Gu, L. Wang, X. C. Ma, and Q. K. Xue, Atomically resolved FeSe/ SrTiO_3 (001) interface structure by scanning transmission electron microscopy, *2D Mater.* **3**, 024002 (2016).
- [52] H. Okabe, N. Takeshita, K. Horigane, T. Muranaka, and J. Akimitsu, Pressure-induced high- T_c superconducting phase in FeSe: Correlation between anion height and T_c , *Phys. Rev. B* **81**, 205119 (2010).
- [53] F. Essenerger, P. Buczek, A. Ernst, L. Sandratskii, and E. K. U. Gross, Paramagnons in FeSe close to a magnetic quantum phase transition: *Ab initio* study, *Phys. Rev. B* **86**, 060412 (2012).
- [54] C. Zhang, L. W. Harriger, Z. Yin, W. Lv, M. Wang, G. Tan, Y. Song, D. L. Abernathy, W. Tian, T. Egami, K. Haule, G. Kotliar, and P. Dai, Effect of Pnictogen Height on Spin Waves in Iron Pnictides, *Phys. Rev. Lett.* **112**, 217202 (2014).
- [55] C. H. Lee, A. Iyo, H. Eisaki, H. Kito, M. T. Fernandez-Diaz, T. Ito, K. Kihou, H. Matsuhata, M. Braden, and K. Yamada, Effect of structural parameters on superconductivity in fluorine-free LnFeAsO_{1-y} ($\text{Ln} = \text{La}, \text{Nd}$), *J. Phys. Soc. Jpn.* **77**, 083704 (2008).